Chinese Journal of
POLYMER SCIENCE

RESEARCH ARTICLE

https://doi.org/10.1007/s10118-024-3177-6
Chinese J. Polym. Sci. **2024**, *42*, 1578–1588

Tough Polymeric Hydrogels Based on Amino Acid Derivative Mediated Dynamic Metal Coordination Bonds

Meng Li[a,†], Meng-Yuan Zhang[a,†], Wu-Xuan Lei[b], Zhu-Ting Lv[a], Qing-Hua Shang[a], Zheng Zhao[c], Jiang-Tao Li[c], and Yi-Long Cheng[a,d*]

[a] *Engineering Research Center of Energy Storage Materials and Devices, Ministry of Education, School of Chemistry, Xi'an Jiaotong University, Xi'an 710049, China*
[b] *Polymer Materials & Engineering Department School of Materials Science & Engineering Chang'an University, Xi'an 710064, China*
[c] *School of Electrical Engineering, Xi'an Jiaotong University, Xi'an 710049, China*
[d] *Department of Nuclear Medicine, the First Affiliated Hospital of China, Xi'an Jiaotong University, Xi'an 710049, China*

Electronic Supplementary Information

Abstract The development of physically crosslinked hydrogels with excellent mechanical and sensing properties is of importance for expanding the practical applications of intelligent soft hydrogel materials. Herein, after copolymerization of hydroxyl-containing amino acid derivative N-acryloyl serine (ASer) with acrylamide (AM), we introduce Zr^{4+} through an immersion strategy to construct metal ion-toughened non-covalent crosslinked hydrogels (with tensile strength of up to 5.73 MPa). It is found that the synergistic coordination of hydroxyl and carboxyl groups with Zr^{4+} substantially increases the crosslinking density of the hydrogels, thereby imparting markedly superior mechanical properties compared to hydroxyl-free Zr^{4+}-crosslinked hydrogels, such as N-acryloyl alanine (AAla) copolymerized with AM hydrogels (with tensile strength of 2.98 MPa). Through the adjustment of the composition of the copolymer and the density of coordination bonds, the mechanical properties of the hydrogels can be modulated over a wide range. Additionally, due to the introduction of metal ions and the dynamic nature of coordination bonds, the hydrogels also exhibit excellent sensing performance and good self-recovery properties, paving the way for the development of flexible electronic substrates with outstanding comprehensive performances.

Keywords Hydrogel; Amino acid; Metal coordination; Mechanical performance; Flexible sensor

Citation: Li, M.; Zhang, M. Y.; Lei, W. X.; Lv, Z. T.; Shang, Q. H.; Zhao, Z.; Li, J. T.; Cheng, Y. L. Tough polymeric hydrogels based on amino acid derivative mediated dynamic metal coordination bonds. *Chinese J. Polym. Sci.* **2024**, *42*, 1578–1588.

INTRODUCTION

Hydrogels are generally regarded as soft and fragile materials, and their poor mechanical properties greatly limit their application as structural elements in biomedical and engineering fields.[1] In contrast, some biological tissues, such as cartilage and tendons, exist in a gel state but exhibit excellent mechanical performance.[2] Therefore, the exploration of soft hydrogels with similar mechanical properties to these natural load-bearing tissues may have a wide range of applications in biomechanical actuators, synthetic cartilage, artificial muscles, ionic skin and soft robots.[3] In recent years, researchers have developed various tough hydrogels with specific network structures and energy dissipation mechanisms, such as double network (DN) hydrogels,[4] double cross-linked hydrogels,[5] nanocomposite (NC) hydrogels,[6] and slide-ring hydrogels.[7] The incorporation of non-covalent interactions into the network as energy dissipation units is currently considered an effective strategy to enhance the toughness of hydrogels.[8] When the materials are stretched or loaded, non-covalent interactions are dissociated before the polymer chain breakage, thus dissipating a significant amount of energy.[9] The incorporation of sacrificial bonds, such as hydrogen bonds,[10] metal coordination bonds,[11] host-guest interactions,[12] ion or Coulomb interactions,[13] into the design of polymer network could effectively achieve the formation of tough hydrogels. Among these strategies, coordination bonds possess high bond energy and can be tuned across a broad spectrum by altering the combination of metal ions and ligands,[14] which also can impart some special properties to hydrogels, including self-healing ability, shape memory behavior, stimulus responsiveness, and high dielectric constants.[15–18] Moreover, the radius and valence state of metal ions have significant effects on the mechanical properties of hydrogels.[19] In recent years, tetravalent metal ions have been widely used to construct metal-coordinated hydrogels due to their strong coordination ability. For example, Wu and co-workers found that Zr^{4+} could form stable coordination bonds with sulfonate and carboxylate groups, thus affording the formation of tough

* Corresponding author, E-mail: yilongcheng@mail.xjtu.edu.cn
† These authors contributed equally to this work.
Special Issue: Dynamic Polymer Networks
Received May 11, 2024; Accepted June 3, 2024; Published online August 28, 2024

supramolecular hydrogels,[20–23] which showed enormous potential in the field of wearable soft electronic device substrates.

Amino acids, as the fundamental components of proteins, are widely distributed in nature and easy to be prepared. With excellent aqueous solubility, tunability, and biocompatibility, it is an ideal candidate for the construction of hydrogels.[24] Additionally, amino acids have multiple active functional groups that can form various non-covalent interactions in water, including the formation of metal-ligand complexes between the polar groups and metal ions.

Our recent study introduced the amino acid derivative, *N*-acryloyl serine acid (ASer) containing hydroxyl group into the design of hydrogel (PASer hydrogel).[25] Leveraging the hydrophilicity of hydroxyl groups, we prepared an injectable and anti-fouling hydrogen-bond crosslinked hydrogel, which showed satisfactory preventive effects on postoperative abdominal adhesions. However, the mechanical properties of the PASer hydrogel were relatively poor. Since oxygen in the hydroxyl group is rich in electrons, we anticipated that the presence of hydroxyl and carboxyl group in ASer may form stable coordination complexes with Zr^{4+}, which could serve as potent crosslinking points in the hydrogel network and endow the resulting hydrogel with excellent mechanical properties.

In this work, we continued to incorporate ASer into the design of hydrogel to explore the coordinating role of hydroxyl functional groups with Zr^{4+}. Specifically, ASer and hydroxyl-free amino acid derivative, *N*-acryloyl alanine (AAla), were copolymerized with acrylamide (AM) to form the initial hydrogels, respectively, which were further incubated with Zr^{4+} to form the coordination bonds toughened hydrogels. The results showed significant differences in the mechanical properties of the types of hydrogels. We hypothesized that the hydroxyl group in ASer also participated in the formation of coordination complexes, which was verified by swelling test, microstructure observation, attenuated total reflectance Fourier transform infrared (ATR-FTIR) and Ramon spectroscopies. We also carefully studied the effect of the concentrations of AM, ASer and Zr^{4+} on the mechanical properties of the hydrogels. Owing to the introduction of metal ions and the dynamic nature of coordination bonds, the hydrogels exhibited good self-recovery performance and excellent sensing capabilities, and the potential as flexible devices for the monitoring of human daily activities and physiological signals was also investigated.

EXPERIMENTAL

Materials

L-serine (Ser), L-alanine (Ala), acryloyl chloride and zirconyl chloride octahydrate ($ZrOCl_2{\cdot}8H_2O$) were provided by Adamas-beta Co., Ltd., and ammonium persulfate (APS, 98%) and *N*,*N*,*N*-tetramethyl ethylene-1,2-diamine (TEMED, 99%) were purchased from Aladdin (Shanghai, China). All other chemicals and solvents used were of analytical grade and did not require additional purification.

Preparation of P(ASer$_x$-AM$_y$)-Zr$^{4+}_z$ Hydrogels

Taking the preparation of P(ASer$_x$-AM$_y$)-Zr$^{4+}_z$ hydrogels as an example, ASer and AM were first dissolved in deionized water at room temperature according to the corresponding concentrations. Then, APS (1.0 wt% of monomers) and TEMED (0.3 wt% of monomers) were added and stirred until completely dissolved. Finally, the solution was injected into a reaction mold composed of a pair of glass plates and a 50 mm × 50 mm × 1 mm silicone rubber spacer, and reacted at 60 °C for 3 h to prepare the hydrogels. The prepared hydrogels were then incubated in $ZrOCl_2$ aqueous solutions of different concentrations for 3 days, followed by transfer to a large amount of pure water for 3 days to reach equilibrium. The P(AAla$_x$-AM$_y$)-Zr$^{4+}_z$ hydrogels were prepared using the same method.

Mechanical Properties

The mechanical performances of the hydrogels were tested on CMT-1503 electromechanical tester (SUST Inc., China) at room temperature. Dumbbell-type samples (16 mm × 4 mm × 1 mm) were tested in tension at a speed of 50 mm·min^{-1} with a 50 N load cell. At least three specimens were tested for each hydrogel sample. The details are shown in Supplemental Materials.

Electrical Test

Electrical tests were conducted by electrochemical workstation CHI 650E (CH Instruments, Inc.). The electrochemical impendence spectroscopy (EIS) of the hydrogels was measured at a test frequency range of 0.1 Hz to 10^6 Hz and 10 mV voltage to obtain the resistance. The relative resistance changes of the hydrogels under different strains were obtained using CMT-1503 electromechanical tester combined with electrochemical workstation CHI 650E. The details are shown in the electronic supplementary information (ESI).

RESULTS AND DISCUSSION

Synthesis of Zr^{4+} Crosslinked Tough Hydrogels

For comparison, two acrylamide monomers, ASer and AAla, were synthesized with minor modifications according to the method in our previous work.[26,27] The two monomers have similar structures, with the only difference being that AAla has one less hydroxyl group than ASer. ^{1}H-NMR and ^{13}C-NMR spectra shown in Figs. S1–S4 (in ESI) indicated the successful production of the two monomers. Correspondingly, P(ASer-AM) and P(AAla-AM) hydrogels were prepared by separately copolymerized with acrylamide (AM) through thermally initiated free radical polymerization (Scheme 1a), and the polymerization process was monitored by ATR-FTIR spectroscopy. As shown in Fig. S5 (in ESI), the disappearance of the bands at 1592 cm^{-1} corresponding to the double bond after reaction for 3 h suggested the completion of the polymerization process.[10] Subsequently, the hydrogels were immersed in $ZrOCl_2$ aqueous solution for 3 days followed by deionized water for 3 days to obtain the tough hydrogels with coordination complexes as crosslinking points (Scheme 1b). The resulting hydrogels were named P(ASer$_x$-AM$_y$)-Zr$^{4+}_z$ and P(AAla$_x$-AM$_y$)-Zr$^{4+}_z$, where *x* and *y* represented the molar concentration of ASer/AAla and AM, respectively, and *z* represented the concentration of the immersed $ZrOCl_2$ aqueous solution.

As shown in Fig. 1(a), the mechanical properties of P(ASer$_{0.4}$-AM$_5$) and P(AAla$_{0.4}$-AM$_5$) hydrogels are relatively poor with tensile strength of about 200 kPa. However, the tensile strength significantly increased to 5.73 and 2.98 MPa after coordination with Zr^{4+}, respectively, indicating the for-

https://doi.org/10.1007/s10118-024-3177-6

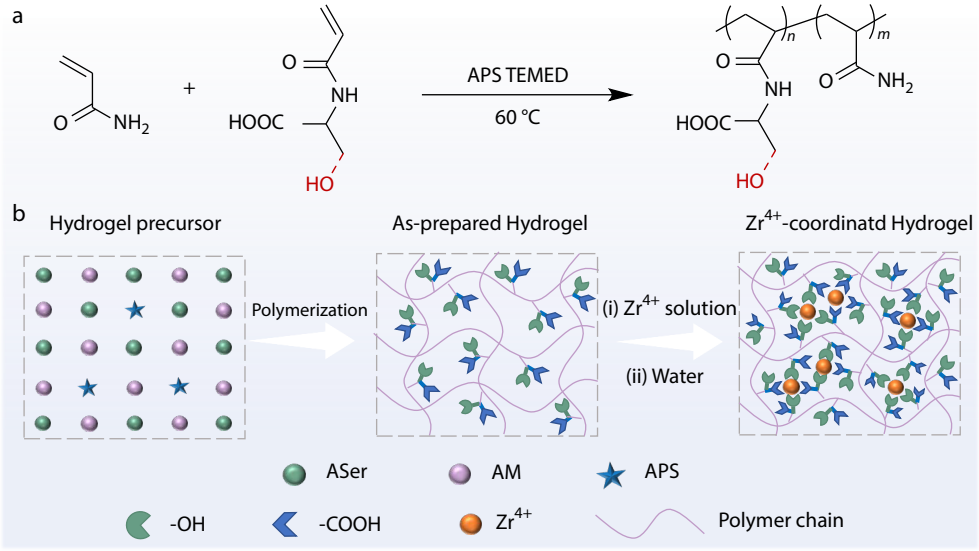

Scheme 1 Scheme of (a) the synthesis of copolymers and (b) Zr^{4+}-reinforced coordination hydrogels.

mation of strong physical crosslinking between the pristine hydrogel and Zr^{4+}. In addition, compared to the P(AAla$_{0.4}$-AM$_5$)-$Zr^{4+}_{0.05}$ hydrogel, the P(ASer$_{0.4}$-AM$_5$)-$Zr^{4+}_{0.05}$ hydrogel exhibited substantial advantages in both tensile strength and elongation at break. The radar chart in Fig. 1(b) quantitatively compared the tensile strength, Young's modulus, maximum strain, and toughness of P(ASer$_{0.4}$-AM$_5$)-$Zr^{4+}_{0.05}$ and P(AAla$_{0.4}$-AM$_5$)-$Zr^{4+}_{0.05}$ hydrogels. It was found that the P(ASer$_{0.4}$-AM$_5$)-$Zr^{4+}_{0.05}$ hydrogel demonstrated superior mechanical performance while maintaining high water content. Moreover, the P(ASer$_{0.4}$-AM$_5$)-$Zr^{4+}_{0.05}$ hydrogel could be stretched to 500% of its original length and withstand 4 kg of weight without breaking. In contrast, the P(AAla$_{0.4}$-AM$_5$)-$Zr^{4+}_{0.05}$ hydrogel could only be stretched to 300% of its original length and could not withstand the weight of 4 kg (Figs. 1c and 1d). This suggested that there may be stronger physical interactions and denser network in the P(ASer$_{0.4}$-AM$_5$)-$Zr^{4+}_{0.05}$ hydrogel. Therefore, we speculated that both carboxyl and hydroxyl groups were involved in the coordination with Zr^{4+} in the P(ASer$_{0.4}$-AM$_5$)-$Zr^{4+}_{0.05}$ hydrogel and increased the crosslinking density of the hydrogel network, which could lead to the increases in the modulus and strength of the hydrogel. Moreover, the metal coordination bonds in the hydrogel network served as sacrificial bonds to endow the hydrogel with effective energy dissipation capability, thereby making the hydrogel with exceptional extensibility.[28,29]

Study on the Coordination of Hydroxyl and Carboxyl Groups with Zr^{4+}

To highlight the positive effect of hydroxyl group on the coordination complexes formation, we first studied the swelling behavior of the P(ASer$_{0.4}$-AM$_5$)-$Zr^{4+}_{0.05}$ and P(AAla$_{0.4}$-AM$_5$)-$Zr^{4+}_{0.05}$ hydrogels. Fig. 2(a) shows the macroscopic photographs of the hydrogels sequentially immersed in $ZrOCl_2$ solution and deionized water, and the swelling kinetics of the hydrogels were monitored by measuring the mass change. As presented in Fig. 2(b), upon immersion of the original P(ASer$_{0.4}$-AM$_5$) and P(AAla$_{0.4}$-AM$_5$) hydrogels in Zr^{4+} solution, the mass of the hydrogels increased rapidly in a short period, and the swelling ratio of P(ASer$_{0.4}$-AM$_5$)-$Zr^{4+}_{0.05}$ hydrogel (105%) was higher than that of P(AAla$_{0.4}$-AM$_5$)-$Zr^{4+}_{0.05}$ hydrogel (76%). Subsequently, the swelling ratio decreased gradually, and the hydrogels began to shrink, essentially returning to their original states by the third day. It was clearly found that the swelling process was much faster than the deswelling process, implying that the construction of metal-ligand coordination bonds took much more time than the de-association of hydrogen bonds. Therefore, when the hydrogels were initially immersed in the solution, there was not enough cross-linking density to resist water permeation with rapid expansion in hydrogel volume.[29] However, as the Zr^{4+} diffused into the gel matrix and interacted with the polar groups, the cross-linking density of the hydrogels increased, thus leading to the gradual shrinkage of hydrogels. Moreover, due to the high swelling ratio of P(ASer$_{0.4}$-AM$_5$)-$Zr^{4+}_{0.05}$ hydrogel in $ZrOCl_2$ solution, more Zr^{4+} permeated into the gel for coordination complexes formation, which led to the low swelling ratio (11%) compared to P(AAla$_{0.4}$-AM$_5$)-$Zr^{4+}_{0.05}$ hydrogel (36%) after further incubation in water for 3 days.

We then employed ATR-FTIR spectroscopy, Roman spectroscopy, scanning electron microscopy (SEM) and X-ray photoelectron spectroscopy (XPS) to analyze the coordination of hydroxyl and carboxyl groups with Zr^{4+}. As shown in Fig. 2(c), the ATR-FTIR spectra reveal that the stretching vibration bands of C=O and C—O for the carboxyl group in P(ASer$_{0.4}$-AM$_5$) and P(AAla$_{0.4}$-AM$_5$) hydrogels shift from 1658 cm^{-1} and 1328 cm^{-1} to 1663 cm^{-1} and 1331 cm^{-1} after crosslinking with Zr^{4+}, respectively, indicating the formation of carboxyl-Zr^{4+} coordination complexes.[21,30,31] Additionally, the band at 1047 cm^{-1} assigned to the stretching vibration of C—O for the hydroxyl group in P(ASer$_{0.4}$-AM$_5$) hydrogel shifted to 1050 cm^{-1} in the spectrum of Zr^{4+}-reinforced P(ASer$_{0.4}$-AM$_5$)-$Zr^{4+}_{0.05}$ hydrogel, suggesting the formation of physical interactions between Zr^{4+} and the hydroxyl group.[32–34] The formation of coordination bonds between Zr^{4+} and carboxyl and hydroxyl group was also reflected in the Raman spectrum. As shown in Fig. 2(d), compared to P(ASer$_{0.4}$-AM$_5$) hydrogel, the characteristic bands of the C=O and C—O (carboxyl group) in the

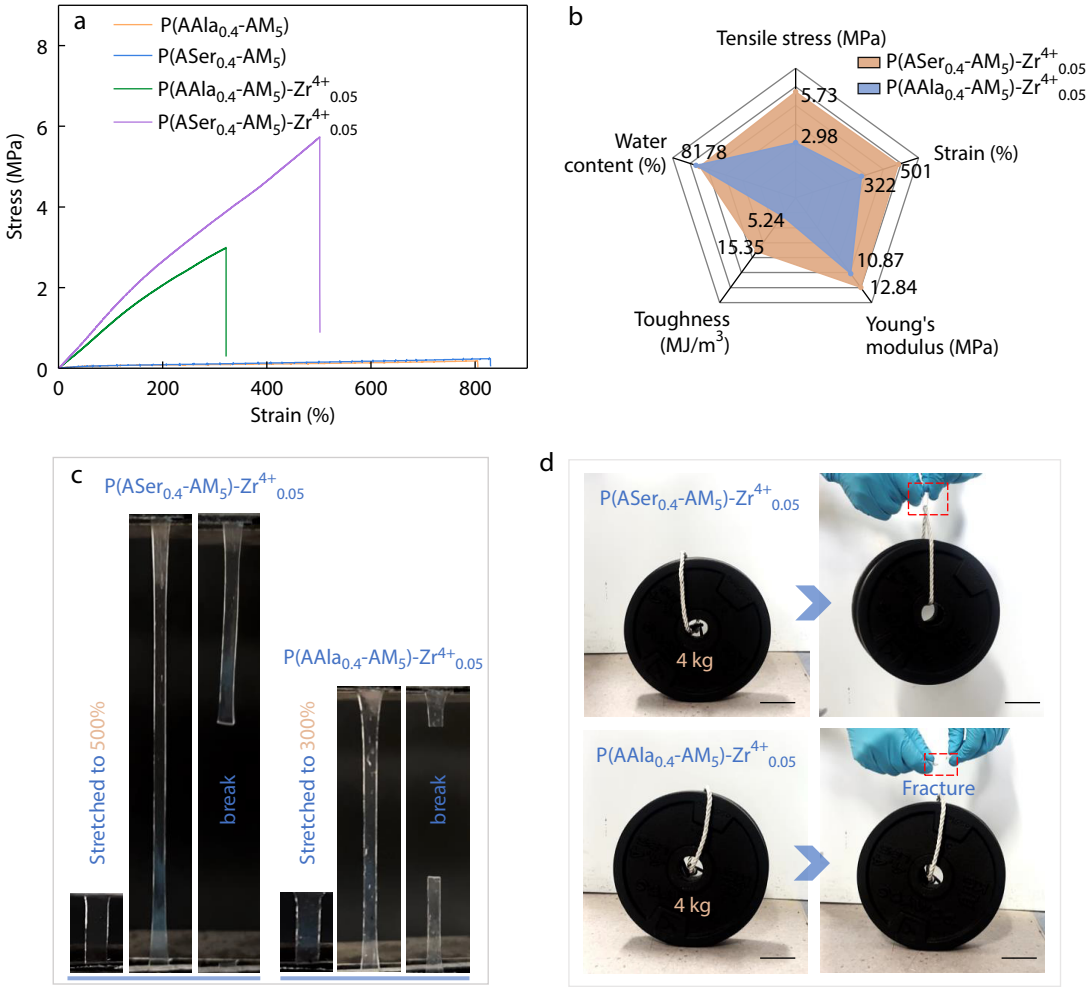

Fig. 1 Comparison of P(ASer$_{0.4}$-AM$_5$)-Zr$^{4+}_{0.05}$ and P(AAla$_{0.4}$-AM$_5$)-Zr$^{4+}_{0.05}$ hydrogels in mechanical properties. (a) Tensile stress-strain curves of P(ASer$_{0.4}$-AM$_5$), P(AAla$_{0.4}$-AM$_5$), P(ASer$_{0.4}$-AM$_5$)-Zr$^{4+}_{0.05}$, and P(AAla$_{0.4}$-AM$_5$)-Zr$^{4+}_{0.05}$ hydrogels. (b) Comparison between P(ASer$_{0.4}$-AM$_5$)-Zr$^{4+}_{0.05}$ and P(AAla$_{0.4}$-AM$_5$)-Zr$^{4+}_{0.05}$ hydrogels in terms of tensile stress, strain, Young's modulus, and toughness. (c-d) Macroscopic comparison photographs of the mechanical properties of P(ASer$_{0.4}$-AM$_5$)-Zr$^{4+}_{0.05}$ and P(AAla$_{0.4}$-AM$_5$)-Zr$^{4+}_{0.05}$ hydrogels. Scale bar: 5 cm.

spectrum of P(ASer$_{0.4}$-AM$_5$)-Zr$^{4+}_{0.05}$ hydrogel shifted from 1650 and 1303 cm^{-1} to 1660 and 1317 cm^{-1}, respectively, and the characteristic band of C—O for the hydroxyl group shifted from 997 cm^{-1} to 1008 cm^{-1}. However, for the P(AAla$_{0.4}$-AM$_5$)-Zr$^{4+}_{0.05}$ hydrogel, only the characteristic bands of C=O and C—O (carboxyl group) shifted from 1650 and 1317 cm^{-1} to 1660 and 1323 cm^{-1} after the introduction of Zr^{4+}, respectively. These results further justified the coordination between Zr^{4+} and hydroxyl groups in the P(ASer$_{0.4}$-AM$_5$)-Zr$^{4+}_{0.05}$ hydrogel.[21,35]

We further used SEM to observe the microstructure of the prepared hydrogels. As depicted in Fig. 2(e), all the four samples show typically porous network structures. The P(ASer$_{0.4}$-AM$_5$) and P(AAla$_{0.4}$-AM$_5$) hydrogels possessed relatively large pore size, whereas the Zr^{4+}-reinforced hydrogels featured compact structure and small pore size, in which the average pore size decreased from 5.96±1.37 μm and 5.65±2.09 μm to 1.82±0.19 μm and 3.49±0.29 μm after the introduction of Zr^{4+}, respectively (Fig. S6 in ESI).[29] Meanwhile, the smallest pore size and the densest structure could be observed for P(ASer$_{0.4}$-AM$_5$)-Zr$^{4+}_{0.05}$ hydrogel, which suggested that the involvement of hydroxyl groups alongside carboxyl groups in the formation of coordination bonds within the P(ASer$_{0.4}$-AM$_5$)-Zr$^{4+}_{0.05}$ hydrogel may effectively densify the hydrogel network.

XPS was further performed to explore the details of the coordinated complexes inside the equilibrium hydrogels. After soaking the hydrogel in $ZrOCl_2$ solution for 3 days, due to the incomplete coordination of Zr^{4+} at this time point, there should exist multiple forms of coordination with hydroxyl and carboxyl groups. Subsequently, after further soaking in deionized water for 3 days, the hydrogel reached an equilibrium state as a result of network structure reorganization and optimization[21]. Elemental analysis in Fig. 2(f) reveals no chloride ions (Cl$^-$) in the gel matrix, which indicated that there was no Cl$^-$ participating in the coordination process although Zr^{4+} ions were introduced in the form of $ZrOCl_2$.[21] The O 1s spectra of the equilibrated hydrogel could be deconvoluted into three peaks located at 530.2, 531.2 and 532.6 eV corresponding to C—O, C—O—Zr and C=O, respectively, among which

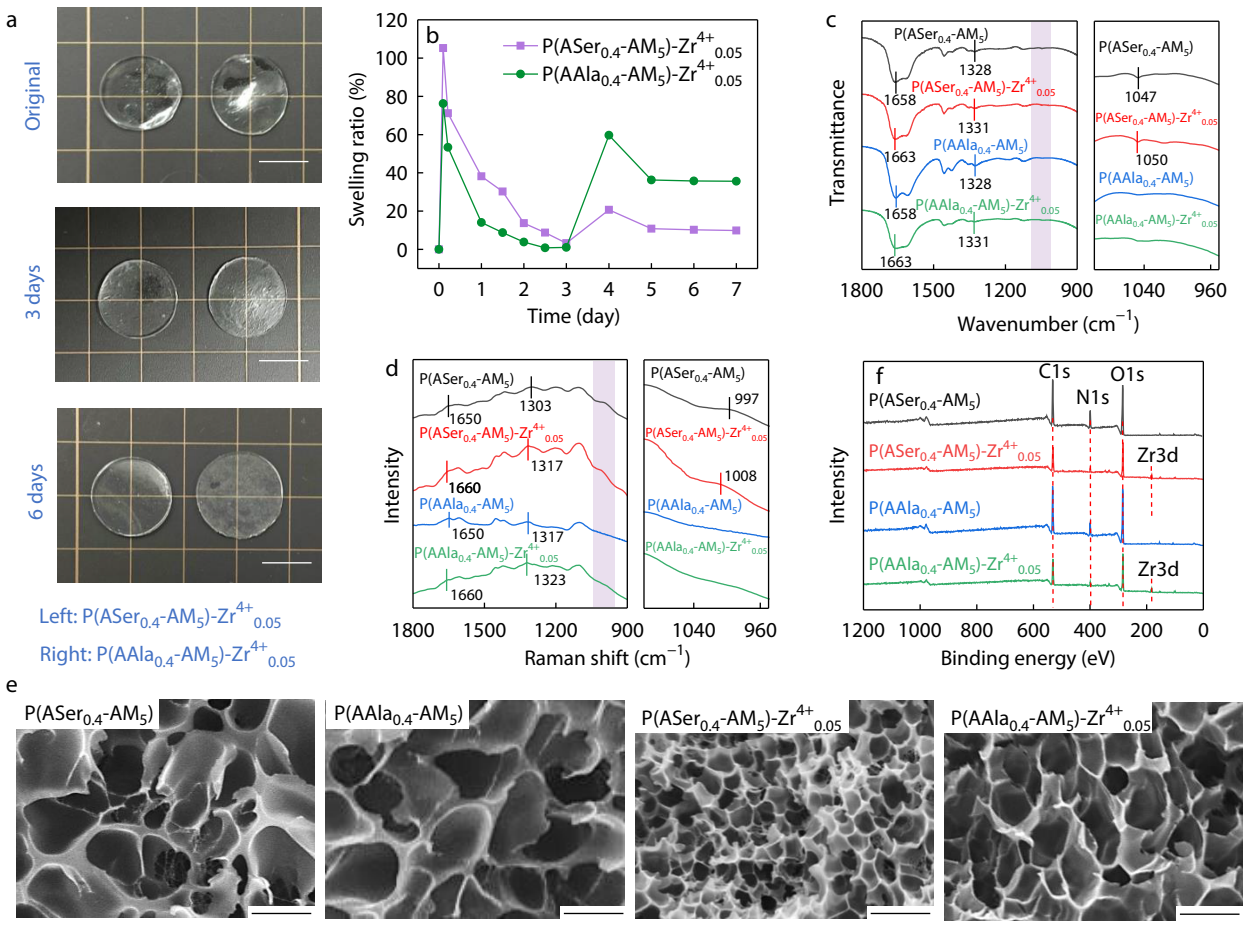

Fig. 2 Evaluation of the coordination of hydroxyl and carboxyl groups with Zr^{4+}. (a) Macroscopic photographs and (b) corresponding swelling ratio of P(ASer$_{0.4}$-AM$_5$)-$Zr^{4+}_{0.05}$ and P(AAla$_{0.4}$-AM$_5$)-$Zr^{4+}_{0.05}$ hydrogels after immersing in $ZrOCl_2$ solution and deionized water sequentially. Scale bar: 5 mm. (c) ATR-FTIR spectra, (d) Raman spectra, (e) SEM images, and (f) XPS full spectra of P(ASer$_{0.4}$-AM$_5$), P(AAla$_{0.4}$-AM$_5$), P(ASer$_{0.4}$-AM$_5$)-$Zr^{4+}_{0.05}$, and P(AAla$_{0.4}$-AM$_5$)-$Zr^{4+}_{0.05}$ hydrogels. Scale bar: 5 μm.

the presence of the C—O—Zr peak suggested the formation of coordination bonds between Zr and O atoms with each Zr surrounded by six O atoms (Figs. S7a and S7b in ESI).[21,36] The deconvoluted Zr 3d peaks showed two binding energies at 182.0 and 184.4 eV, which corresponded to Zr $3d_{5/2}$ and Zr $3d_{3/2}$, respectively (Figs. S7c and S7d in ESI).[37] The area ratio of these two peaks is consistently≈2:3 with a spin-orbit separation of 2.4 eV, which is a typical characteristic of Zr^{4+} in a fully oxidized state and suggested no redox during the coordination process.[8,38]

Mechanical Properties of P(ASer$_x$-AM$_y$)-Zr^{4+}_z Hydrogels

The concentrations of ASer, AM and Zr^{4+} could affect the content of the coordination complexes in the polymer network and further the hydrogel mechanical properties. As shown in Figs. 3(a) and 3(b), the concentration of ASer (C_{ASer}) greatly influences the mechanical properties of P(ASer$_x$-AM$_y$)-Zr^{4+}_z hydrogels. As the C_{ASer} increased from 0.05 mol/L to 0.6 mol/L, the tensile strength (σ_b), elongation at break (ε_b), and fracture toughness (T) of the hydrogels first increased and then decreased with maximum values of 5.73 MPa, 501%, and 15.35 MJ·m^{-3} at C_{ASer} of 0.4 mol/L, respectively, while the Young's modulus (E) continuously increased from 0.55 MPa to 15.57 MPa. The improved mechanical performances of the hydrogels with high C_{ASer} resulted from the increased densities of polymer chains and physical crosslinks.[21] Because the fast coordination process could result in the compact surface layer inhibiting further diffusion of Zr^{4+} into the central region, the successive increment of C_{ASer} might lead to a heterogeneous structure of the gel.[39] This phenomenon would increase the inhomogeneity of the network structure and brittleness of the hydrogel. When C_{ASer} reached 0.6 mol/L, delaminated layers were even found in the hydrogel. Although hydrogels prepared with high C_{ASer} exhibited high stiffness, the water content (q) could still be maintained above 70 wt%. Table S1 (in ESI) summarized the mechanical properties and water content of hydrogels with different C_{ASer}.

We further varied the concentration of AM in the following experiments to investigate the change of mechanical performances for the hydrogels (C_{ASer} was set as 0.4 mol/L). As shown in Figs. 3(c) and 3(d), when C_{AM} is lower than 4 mol/L, the hydrogel was fragile with ε_b lower than 200%. As C_{AM} increased from 4 mol/L to 6 mol/L, ε_b increased to 515%, while σ_b, E, and T initially increased and then decreased with maximum values of 5.73 MPa, 12.84 MPa and 15.35 MJ·m^{-3} at C_{AM} of 5 mol/L, respectively. The high extensibility of polymers always requires dynamic interactions and flexible chain movements, while high strength typically derives from abundant

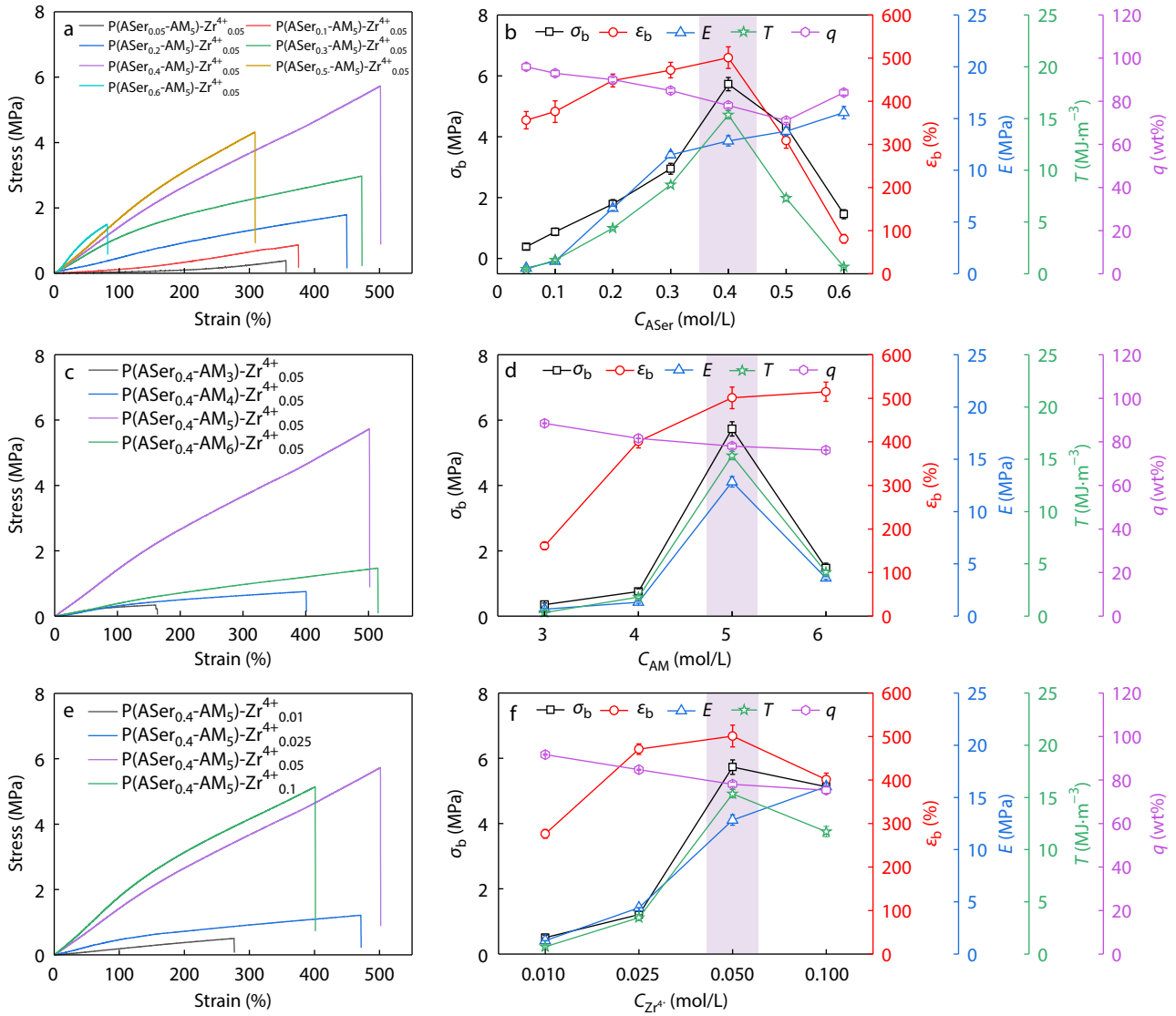

Fig. 3 Mechanical properties of P(ASer$_x$-AM$_y$)-Zr$^{4+}{}_z$ hydrogels. (a) Tensile stress-strain curves and (b) corresponding mechanical properties of the P(ASer$_x$-AM$_5$)-Zr$^{4+}{}_{0.05}$ hydrogels with different C_{ASer}. (c) Tensile stress-strain curves and (d) corresponding mechanical properties of the P(ASer$_{0.4}$-AM$_y$)-Zr$^{4+}{}_{0.05}$ hydrogels with different C_{AM}. (e) Tensile stress-strain curves and (f) corresponding mechanical properties of the P(ASer$_{0.4}$-AM$_5$)-Zr$^{4+}{}_z$ hydrogels with different $C_{Zr^{4+}}$.

cross-linking sites and rigid polymer segments.[40] Therefore, AM as a flexible chain segment would increase the polymer density and chain entanglement to a certain extent with the increase of C_{AM}, thereby improving the comprehensive performance of hydrogels.[20] However, as C_{AM} further increased, the additional flexible polymer chains would weaken the rigidity of the gel, resulting in a decrease in the strength and modulus of the hydrogel. Additionally, these tough hydrogels had high water content, which only slightly decreased from 88 wt% to 76 wt% with the increment in C_{AM}. Table S2 (in ESI) summarizes the mechanical properties and water content of hydrogels with different C_{AM}.

The density of metal coordination bonds was further adjusted by changing the concentration of the soaking Zr^{4+} solution ($C_{Zr^{4+}}$). As shown in Figs. 3(e) and 3(f), P(ASer$_{0.4}$-AM$_5$)-Zr$^{4+}{}_z$ hydrogels are remarkably toughened through the incubation in solutions with different $C_{Zr^{4+}}$; as $C_{Zr^{4+}}$ increased from 0.01 mol/L to 0.1 mol/L, E of the equilibrium hydrogels increased from 1.28 MPa to 16.05 MPa, yet σ_b, ε_b, and T raised first and then declined, which reached the maximum values of 5.73 MPa, 501%, and 15.35 MJ·m^{-3} at $C_{Zr^{4+}}$ of 0.05 mol/L, respectively. This behavior could be explained by the fact that the increase in Zr^{4+} content enhanced the crosslinking density of the hydrogels; however, excessive crosslinking inevitably restricted the mobility of polymer chains and resulted in a decrease in stretchability.[23] Table S3 (in ESI) summarizes the mechanical properties and water content of hydrogels with different $C_{Zr^{4+}}$. Moreover, we tested the changes in the mechanical properties of P(ASer$_{0.4}$-AM$_5$)-Zr$^{4+}{}_{0.05}$ hydrogel through the extension of incubation time. It was found that the P(ASer$_{0.4}$-AM$_5$)-Zr$^{4+}{}_{0.05}$ hydrogel could maintain excellent mechanical stability after long-term incubation in water. As shown in Fig. S8 (in ESI), although gradual increase in Young's modulus (E) and decrease in elongation at break (ε_b) with pro-

https://doi.org/10.1007/s10118-024-3177-6

longed immersion time at room temperature were detected, the tensile strength (σ_b) remained relatively stable. The reinforcement in modulus could be attributed to the gradual reconstruction of Zr^{4+} in water and the structural optimization of the crosslinked network.

As described above, the mechanical properties of the tough hydrogels could be tailored over a wide range by modulating the content of copolymers and the density of metal coordination bonds. Considering the combined mechanical performances, the equilibrated P(ASer$_{0.4}$-AM$_5$)-$Zr^{4+}_{0.05}$ hydrogel was selected to investigate further properties and applications.

Elasticity, Recoverability, and Fatigue Resistance of the P(ASer$_{0.4}$-AM$_5$)-$Zr^{4+}_{0.05}$ Hydrogel

The incorporation of dynamic and reversible physical interac-

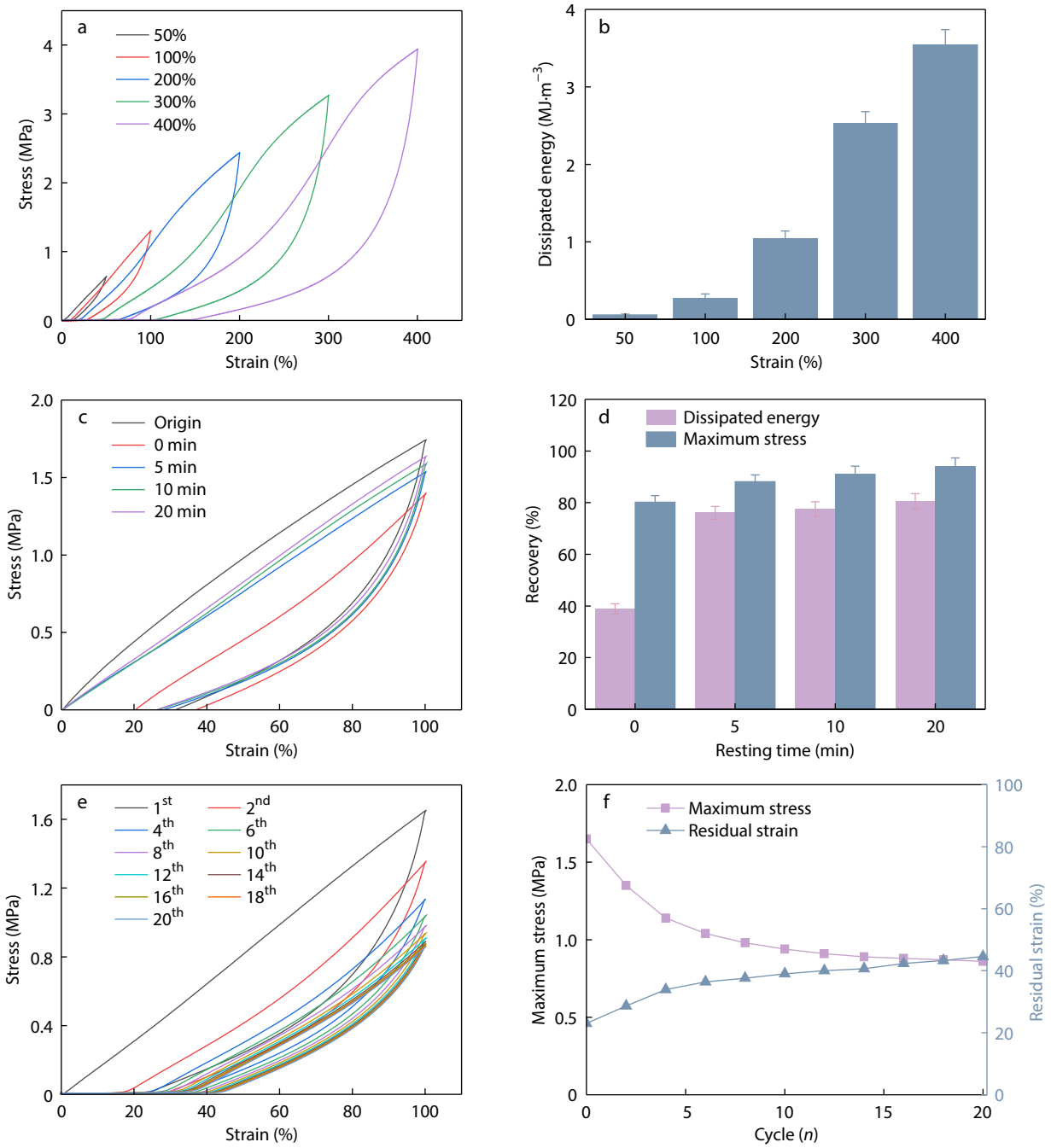

Fig. 4 Elasticity, recoverability, and fatigue resistance of the P(ASer$_{0.4}$-AM$_5$)-$Zr^{4+}_{0.05}$ hydrogel. (a) The loading-unloading curves of P(ASer$_{0.4}$-AM$_5$)-$Zr^{4+}_{0.05}$ hydrogel with various strains and (b) the corresponding dissipative energy; (c) The loading-unloading curves of P(ASer$_{0.4}$-AM$_5$)-$Zr^{4+}_{0.05}$ hydrogel with different recovery time at the strain of 100% and (d) the corresponding recovery ratio; (e) The continuous loading-unloading cyclic curves of P(ASer$_{0.4}$-AM$_5$)-$Zr^{4+}_{0.05}$ hydrogel at 100% strain and (f) the corresponding variation of maximum stress and residual strain with stretching cycles.

https://doi.org/10.1007/s10118-024-3177-6

tions (hydrogen bonding and coordination interactions) endows the P($ASer_{0.4}$-AM_5)-$Zr^{4+}_{0.05}$ hydrogel with effective energy dissipation capability.[41–43] The dissipation energy of the P($ASer_{0.4}$-AM_5)-$Zr^{4+}_{0.05}$ hydrogel was investigated through typical loading-unloading experiments. As presented in Fig. 4(a), the area of the hysteresis loop become larger with increased strain in the cyclic stretching experiment, indicating a gradual increase in the degree of damage to the internal network structure preceded by macroscopic fracture.[41] Additionally, the overlapped regions between any adjacent hysteresis loops were observed, which also indicated the good self-recovery capability of the hydrogel.[41] As the strain increased gradually from 50% to 400%, the dissipated energy continuously increased from 0.058 MJ·m^{-3} to 3.54 MJ·m^{-3} (Fig. 4b), implying more energy dissipated owing to the gradual dissociation of coordination bonds during deformation. Since the P($ASer_{0.4}$-AM_5)-$Zr^{4+}_{0.05}$ hydrogel is crosslinked by multiple dynamic non-covalent bonds, it is expected to rebuild and recover rapidly to maintain stability in successive cycles once external stress is released for practical applications.[44–45] We evaluated the self-recovery performance of the P($ASer_{0.4}$-AM_5)-$Zr^{4+}_{0.05}$ hydrogel through cyclic tensile tests with different relaxation times at room temperature. As shown in Fig. 4(c), the P($ASer_{0.4}$-AM_5)-$Zr^{4+}_{0.05}$ hydrogel exhibits apparent hysteresis loop with a larger dissipated energy in the first loading-unloading cycle; the dissipative energy and maximum stress of the immediate test was 39% and 80% of the initial values, respectively. With the extension of the time interval, the P($ASer_{0.4}$-AM_5)-$Zr^{4+}_{0.05}$ hydrogel showed a gradual restoration in dissipative energy and maximum stress, which recovered to 80% and 94% after waiting for 20 min (Fig. 4d), respectively. Next, 20 successive loading-unloading cyclic tests were carried out under 100% strain to assess the antifatigue capability of the P($ASer_{0.4}$-AM_5)-$Zr^{4+}_{0.05}$ hydrogel. As depicted in Fig. 4(e), a pronounced hysteresis loop can be observed in the first cycle, which suggested partial dissociation of hydrogen bonds and metal coordination bonds within the hydrogel network.[41,46] However, in the subsequent cycles, the area of the hysteresis loop gradually diminished, and there is no apparent change in the maximum stress and residual strain of the hydrogel, suggesting that the P($ASer_{0.4}$-AM_5)-$Zr^{4+}_{0.05}$ hydrogel possessed good fatigue resistance (Fig. 4f).

Conductivity and Sensing Properties of the P($ASer_{0.4}$-AM_5)-$Zr^{4+}_{0.05}$ Hydrogel

In addition to the enhancement in the mechanical performance, the introduction of metal ions also endows P($ASer_{0.4}$-AM_5)-$Zr^{4+}_{0.05}$ hydrogel with excellent conductivity and electrical sensitivity.[47] Since the P($ASer_{0.4}$-AM_5)-$Zr^{4+}_{0.05}$ hydrogel possessed porous microstructure with water content exceeding 70%, the high mobility of residual uncoordinated ions (such as Zr^{4+} and COO^-) should be allowed in the hydrogel matrix, thereby leading to excellent ion conductivity.[41,48] As a proof of concept, the P($ASer_{0.4}$-AM_5)-$Zr^{4+}_{0.05}$ hydrogel as conductor was connected to a complete circuit to observe the change of LED brightness after stretching. As shown in Fig. S9 (in ESI), the stretch of the P($ASer_{0.4}$-AM_5)-$Zr^{4+}_{0.05}$ hydrogel could lead to diminution in the brightness of the LED due to the narrowing and elongation of the conducting pathway. Upon release of the external force, the brightness of LED returned to a normal state. We further employed electrochemical impedance spectroscopy (EIS) to determine the conductivity of P($ASer_{0.4}$-AM_5)-Zr^{4+}_{z} hydrogels immersed in $ZrOCl_2$ solutions with different concentrations (Fig. 5a), and the *x*-axis intercepts of the curves in Nyquist plots corresponded to the impedance of the hydrogels (illustration of Fig. 5a).[49] The results indicated that with the increment of Zr^{4+} concentration, the impedance of P($ASer_{0.4}$-AM_5)-Zr^{4+}_{z} hydrogels gradually decreased and the conductivity increased, in which the conductivity of P($ASer_{0.4}$-AM_5)-$Zr^{4+}_{0.1}$ hydrogel could reach 0.19 S·m^{-1}. Under deformation, the changes in ion transport channel and length can result in variations in conductivity, enabling hydrogels to be used as strain sensors.[50,51] Gauge factor (GF), a parameter represented the sensitivity of strain sensors, reflecting the change in relative resistance with applied strain, was divided into three stages according to strain for the P($ASer_{0.4}$-AM_5)-$Zr^{4+}_{0.05}$ hydrogel.[52] As depicted in Fig. S10 (in ESI), the GF value was 0.56, 0.60, and 1.52 in the strain range of 0%–100%, 100%–200%, and 200%–300%, respectively. Typically, the maximum deformation of the skin during various human movements was about 75%, thus the application of hydrogel sensors in monitoring human motion was reliable.[41]

We then examined the sensing capability of the P($ASer_{0.4}$-AM_5)-$Zr^{4+}_{0.05}$ hydrogel through real-time monitoring of relative resistance changes. As illustrated in Figs. 5(b) and 5(c), the hydrogel sensor could accurately and sensitively detect $\Delta R/R_0$ during repeated stretching processes at low (2% to 10%) and high strain ranges (50% to 200%), and the obtained peak values were continuous and distinguishable with proportional increase in the relative resistance changes. Moreover, the change of the stretching rate (from 10 mm to 40 mm·min^{-1}) under a fixed strain of 100% did not affect the outputted electrical signals, demonstrating the rate-independent characteristics and high stability (Fig. 5d). Subsequently, to validate the reliability of monitoring continuous human movement, the amplitude of the resistance signal was tracked during 50 loading-unloading cycles with a fixed strain of 50%. As shown in Fig. S11 (in ESI), the relative resistance change remained relatively stable throughout the continuous cycles, which indicated that the P($ASer_{0.4}$-AM_5)-$Zr^{4+}_{0.05}$ hydrogel as strain sensor is reliable for long-term applications.

Sensing Performances of the P($ASer_{0.4}$-AM_5)-$Zr^{4+}_{0.05}$ Hydrogel

Based on the above results, the P($ASer_{0.4}$-AM_5)-$Zr^{4+}_{0.05}$ hydrogel exhibited unique sensing performance, high sensitivity, and a wide operating range, which made it suitable as wearable sensors to monitor human activities in real-time. For the movements of the wrist, neck, elbow, and knee joints, the P($ASer_{0.4}$-AM_5)-$Zr^{4+}_{0.05}$ hydrogel could output corresponding signals for identification. It could be observed from Fig. 5(e) that there is an obvious change in resistance when the hydrogel strain sensor was attached to the wrist; Fig. 5(f) illustrates the movement of the neck joint for health management, by which the bowing head could be constantly reflected by the elevation of electrical signals. Additionally, the hydrogel sensor could also monitor the movement of the arms and walking process in real time (Fig. S12 in ESI). In these movements, the hydrogel was under tension state, which resulted in an increase in resistance due to the elongation of the conductive pathways with positive output electrical signals.

To further demonstrate its potential for involvement in var-

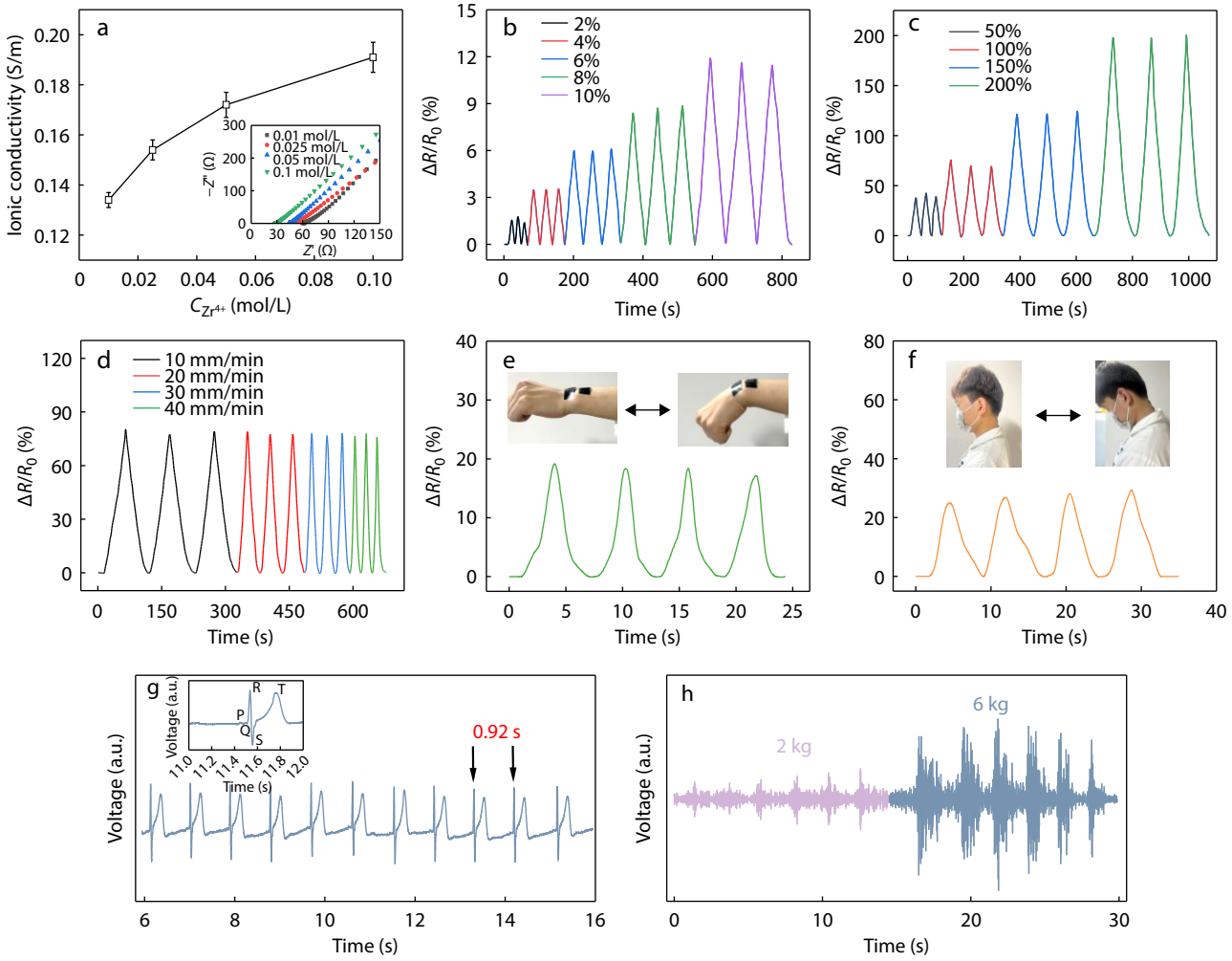

Fig. 5 Conductivity and sensing properties of P(ASer$_{0.4}$-AM$_5$)-Zr$^{4+}_{0.05}$ hydrogels. (a) Ionic conductivity of P(ASer$_{0.4}$-AM$_5$)-Zr$^{4+}_z$ hydrogels with various Zr^{4+} content; (b,c) Relative resistance changes of P(ASer$_{0.4}$-AM$_5$)-Zr$^{4+}_{0.05}$ hydrogel with small strains (2%–10%) (b) and large strains (50%–200%) (c). (d) Relative resistance changes of P(ASer$_{0.4}$-AM$_5$)-Zr$^{4+}_{0.05}$ hydrogel at different stretching rates with 100% strain; (e,f) Relative resistance changes of P(ASer$_{0.4}$-AM$_5$)-Zr$^{4+}_{0.05}$ hydrogel as a strain sensor to detect various human motions: wrist bending (e) and neck bending (f). (g,h) ECG (g) and EMG (h) monitoring using P(ASer$_{0.4}$-AM$_5$)-Zr$^{4+}_{0.05}$ hydrogel electrode.

ious types of sensors, the P(ASer$_{0.4}$-AM$_5$)-Zr$^{4+}_{0.05}$ hydrogel was assembled as skin electrode to detect pressure changes that correlate to electrophysiological signals, such as electrocardiograms (ECG) and electromyograms (EMG).[53,54] As shown in Fig. 5(g), the ECG signals recorded with the P(ASer$_{0.4}$-AM$_5$)-Zr$^{4+}_{0.05}$ hydrogel electrode exhibit clear PQRST waveforms, and the time delay between the two consecutive S peaks was approximately 0.92 s with relevant heart rate of 65 beats per minute, which is in the regular range (60–100 beats/min) for an adult.[54] Similar experiments were conducted to evaluate the EMG monitoring capability of the P(ASer$_{0.4}$-AM$_5$)-Zr$^{4+}_{0.05}$ hydrogel electrode (Fig. 5h), and the changes in the bioelectric potential caused by the transition between the relaxed and tense state of the flexor carpi were recorded. The P(ASer$_{0.4}$-AM$_5$)-Zr$^{4+}_{0.05}$ hydrogel electrode could monitor stable EMG signals when gripping with different forces, and the EMG signals intensity increased with the corresponding grip force, which could be used for postoperative muscle rehabilitation training. These results demonstrated that the P(ASer$_{0.4}$-AM$_5$)-Zr$^{4+}_{0.05}$ hydrogel-based epidermal sensor showed vast potential for intelligent sensing applications.

CONCLUSIONS

In this study, we reported the preparation of tough polymer hydrogels through the formation of potent Zr^{4+}-based coordination complexes in the network. Compared to the hydroxyl group-free AAla, the copolymerization of ASer and AM in water followed by the incubation in $ZrOCl_2$ aqueous solution could obviously elevate the comprehensive mechanical properties of the resulting hydrogels. Detailed studies demonstrated the presence of hydroxyl group in ASer could also coordinate with Zr^{4+} to improve the crosslinking density of the P(ASer$_{0.4}$-AM$_5$)-Zr$^{4+}_{0.05}$ hydrogel. Moreover, the mechanical properties of the hydrogels were broadly tunable and precisely controllable by adjusting the concentrations of ASer, AM, and Zr^{4+}. The coordination complexes-based hydrogels also exhibited excellent self-recovery and sensing capabilities, which may be a good candidate in the field of wearable soft electronic device substrates.

https://doi.org/10.1007/s10118-024-3177-6

Conflict of Interests

The authors declare no interest conflict.

Electronic Supplementary Information

Electronic supplementary information (ESI) is available free of charge in the online version of this article at http://doi.org/10.1007/s10118-024-3177-6.

Data Availability Statement

The data are available from the corresponding author on reasonable request.

ACKNOWLEDGMENTS

This work was financially supported by the National Natural Science Foundation of China (Nos. 52322309 and 52173139), the "Young Talent Support Plan" of Xi'an Jiaotong University, and Fundamental Research Funds for the Central Universities (No. xzy022023018).

REFERENCES

1 Zhang, Y. S.; Khademhosseini, A. Advances in engineering hydrogels. *Science* **2017**, *356*, eaaf3627.
2 Wegst, U. G. K.; Ashby, M. F. The mechanical efficiency of natural materials. *Philos. Mag.* **2004**, *84*, 2167–2186.
3 Huang, H.; Dong, Z.; Ren, X.; Jia, B.; Li, G.; Zhou, S.; Zhao, X.; Wang, W. High-strength hydrogels: fabrication, reinforcement mechanisms, and applications. *Nano Res.* **2023**, *16*, 3475–3515.
4 Gong, J. P.; Katsuyama, Y.; Kurokawa, T.; Osada, Y. Double-network hydrogels with extremely high mechanical strength. *Adv. Mater.* **2003**, *15*, 1155–1158.
5 Liu, J.; Tan, C. S. Y.; Yu, Z.; Li, N.; Abell, C.; Scherman, O. A. Tough supramolecular polymer networks with extreme stretchability and fast room-temperature self-healing. *Adv. Mater.* **2017**, *29*, 1605325.
6 Wang, J.; Lin, L.; Cheng, Q.; Jiang, L. A strong bio-inspired layered PNIPAM–clay nanocomposite hydrogel. *Angew. Chem. Int. Ed.* **2012**, *51*, 4676–4680.
7 Okumura, Y.; Ito, K. The Polyrotaxane Gel: A Topological Gel by Figure-of-Eight Cross-links. *Adv. Mater.* **2001**, *13*, 485–487.
8 Hu, J. Y.; Jiao, D.; Hao, X. P.; Kong, X.; Zhang, X. N.; Du, M.; Zheng, Q.; Wu, Z. L. A facile strategy to fabricate tough and adhesive elastomers by *in situ* formation of coordination complexes as physical crosslinks. *Adv. Funct. Mater.* **2023**, *33*, 2307402.
9 Sun, T. L.; Kurokawa, T.; Kuroda, S.; Ihsan, A. B.; Akasaki, T.; Sato, K.; Haque, M. A.; Nakajima, T.; Gong, J. P. Physical hydrogels composed of polyampholytes demonstrate high toughness and viscoelasticity. *Nat. Mater.* **2013**, *12*, 932–937.
10 Zhang, M.; Yu, J.; Shen, K.; Wang, R.; Du, J.; Zhao, X.; Yang, Y.; Xu, K.; Zhang, Q.; Zhang, Y.; Cheng, Y. Highly stretchable nanocomposite hydrogels with outstanding antifatigue fracture based on robust noncovalent interactions for wound healing. *Chem. Mater.* **2021**, *33*, 6453–6463.
11 Lai, J. C.; Jia, X. Y.; Wang, D. P.; Deng, Y. B.; Zheng, P.; Li, C. H.; Zuo, J. L.; Bao, Z. Thermodynamically stable whilst kinetically labile coordination bonds lead to strong and tough self-healing polymers. *Nat. Commun.* **2019**, *10*, 1164.
12 Zhang, Z.; Zhao, J.; Guo, Z.; Zhang, H.; Pan, H.; Wu, Q.; You, W.; Yu, W.; Yan, X. Mechanically interlocked networks cross-linked by a molecular necklace. *Nat. Commun.* **2022**, *13*, 1393.
13 Nie, F. M.; An, C. H.; Cao, D. F.; Liu, J.; Zhou, Y. F.; Lu, Y. G.; Ma, Z.; Pan, L.; Li, Y. S. Ru(II) catalyst enables dynamic dual-cross-linked elastomers with near-infrared self-healing toward flexible electronics. *Adv. Funct. Mater.* **2021**, *32*, 2110616.
14 Li, C. H.; Zuo, J. L. Self-healing polymers based on coordination bonds. *Adv. Mater.* **2019**, *32*, 1903762.
15 Lai, J. C.; Li, L.; Wang, D. P.; Zhang, M. H.; Mo, S. R.; Wang, X.; Zeng, K. Y.; Li, C. H.; Jiang, Q.; You, X. Z.; Zuo, J. L. A rigid and healable polymer cross-linked by weak but abundant Zn(II)-carboxylate interactions. *Nat. Commun.* **2018**, *9*, 2725.
16 Tang, Z.; Huang, J.; Guo, B.; Zhang, L.; Liu, F. Bioinspired engineering of sacrificial metal-ligand bonds into elastomers with supramechanical performance and adaptive recovery. *Macromolecules* **2016**, *49*, 1781–1789.
17 Li, M.; Lyu, Q.; Sun, L.; Peng, B.; Zhang, L.; Zhu, J. Fluorescent metallosupramolecular elastomers for fast and ultrasensitive humidity sensing. *ACS Appl. Mater. Interfaces* **2020**, *12*, 39665–39673.
18 Rao, Y. L.; Chortos, A.; Pfattner, R.; Lissel, F.; Chiu, Y. C.; Feig, V.; Xu, J.; Kurosawa, T.; Gu, X.; Wang, C.; He, M.; Chung, J. W.; Bao, Z. Stretchable self-healing polymeric dielectrics cross-linked through metal-ligand coordination. *J. Am. Chem. Soc.* **2016**, *138*, 6020–6027.
19 Yang, C. H.; Wang, M. X.; Haider, H.; Yang, J. H.; Sun, J.-Y.; Chen, Y. M.; Zhou, J.; Suo, Z. Strengthening alginate/polyacrylamide hydrogels using various multivalent cations. *ACS Appl. Mater. Interfaces* **2013**, *5*, 10418–10422.
20 Yu, H. C.; Li, C. Y.; Du, M.; Song, Y.; Wu, Z. L.; Zheng, Q. Improved toughness and stability of κ-carrageenan/polyacrylamide double-network hydrogels by dual cross-linking of the first network. *Macromolecules* **2019**, *52*, 629–638.
21 Yu, H. C.; Hao, X. P.; Zhang, C. W.; Zheng, S. Y.; Du, M.; Liang, S.; Wu, Z. L.; Zheng, Q. Engineering tough metallosupramolecular hydrogel films with Kirigami structures for compliant soft electronics. *Small* **2021**, *17*, 2103836.
22 Zheng, S. Y.; Shen, Y.; Zhu, F.; Yin, J.; Qian, J.; Fu, J.; Wu, Z. L.; Zheng, Q. Programmed deformations of 3D-printed tough physical hydrogels with high response speed and large output force. *Adv. Funct. Mater.* **2018**, *28*, 1803366.
23 Yu, H. C.; Zheng, S. Y.; Fang, L.; Ying, Z.; Du, M.; Wang, J.; Ren, K. F.; Wu, Z. L.; Zheng, Q. Reversibly transforming a highly swollen polyelectrolyte hydrogel to an extremely tough one and its application as a tubular grasper. *Adv. Mater.* **2020**, *32*, 2005171.
24 Dou, X. Q.; Feng, C. L. Amino acids and peptide-based supramolecular hydrogels for three-dimensional cell culture. *Adv. Mater.* **2017**, *29*, 1604062.
25 Li, M.; Zhang, M.; Liu, Z.; Xie, R.; Yang, Y.; Shen, K.; Yang, A.; Cheng, Y. Injectable and self-fused hydrogels with antifouling capability based on amino acid derivatives for postoperative anti-adhesion application. *Sci. China Mater.* **2024**, *67*, 1521–1532.
26 Yu, J.; Xu, K.; Chen, X.; Zhao, X.; Yang, Y.; Chu, D.; Xu, Y.; Zhang, Q.; Zhang, Y.; Cheng, Y. Highly stretchable, tough, resilient, and antifatigue hydrogels based on multiple hydrogen bonding interactions formed by phenylalanine derivatives. *Biomacromolecules* **2021**, *22*, 1297–1304.
27 Yu, J.; Qin, Y.; Yang, Y.; Zhao, X.; Zhang, Z.; Zhang, Q.; Su, Y.; Zhang, Y.; Cheng, Y. Robust hydrogel adhesives for emergency rescue and gastric perforation repair. *Bioact. Mater.* **2023**, *19*, 703–716.
28 Filippidi, E.; Cristiani, T. R.; Eisenbach, C. D.; Waite, J. H.; Israelachvili, J. N.; Ahn, B. K.; Valentine, M. T. Toughening elastomers using mussel-inspired iron-catechol complexes.

Science **2017**, *358*, 502–505.
29 Huang, Y.; Xiao, L.; Zhou, J.; Liu, T.; Yan, Y.; Long, S.; Li, X. Strong tough polyampholyte hydrogels *via* the synergistic effect of ionic and metal-ligand bonds. *Adv. Funct. Mater.* **2021**, *31*, 2103917.
30 Zheng, S. Y.; Ding, H.; Qian, J.; Yin, J.; Wu, Z. L.; Song, Y.; Zheng, Q. Metal-coordination complexes mediated physical hydrogels with high toughness, stick-slip tearing behavior, and good processability. *Macromolecules* **2016**, *49*, 9637–9646.
31 Dou, X.; Wang, H.; Yang, F.; Shen, H.; Wang, X.; Wu, D. One-step soaking strategy toward anti-swelling hydrogels with a stiff "armor". *Adv. Sci.* **2023**, *10*, 2206242.
32 Chen, B.; Chen, Q.; Xiao, S.; Feng, J.; Zhang, X.; Wang, T. Giant negative thermopower of ionic hydrogel by synergistic coordination and hydration interactions. *Sci. Adv.* **2021**, *7*, eabi7233.
33 Song, P.; Xu, Z.; Dargusch, M. S.; Chen, Z. G.; Wang, H.; Guo, Q. Granular nanostructure: a facile biomimetic strategy for the design of supertough polymeric materials with high ductility and strength. *Adv. Mater.* **2017**, *29*, 1704661.
34 Zhao, Z.; Fan, X.; Wang, S.; Jin, X.; Li, J.; Wei, Y.; Wang, Y. Natural polymers-enhanced double-network hydrogel as wearable flexible sensor with high mechanical strength and strain sensitivity. *Chinese Chem. Lett.* **2023**, *34*, 107892.
35 Murugan, D.; Arumugam, H.; Arumugam, S.; Mani, M.; Kannan, S. Superparamagnetic freeze-thawed PVA hydrogel for applications in tissue engineering, drug delivery and bioimaging. *Colloids Surf. A: Physicochem. Eng. Asp.* **2024**, *690*, 133790.
36 Sormani, G.; Korde, A.; Rodriguez, A.; Denecke, M.; Hassanali, A. Zirconium coordination chemistry and its role in optimizing hydroxymate chelation: insights from molecular dynamics. *ACS Omega* **2023**, *8*, 36032–36042.
37 Liu, D.; Jiang, P.; Wang, Y.; Lu, Y.; Wu, J.; Xu, X.; Ji, Z.; Sun, C.; Wang, X.; Liu, W. Engineering tridimensional hydrogel tissue and organ phantoms with tunable springiness. *Adv. Funct. Mater.* **2023**, *33*, 2214885.
38 Tan, Z.; Li, S.; Wang, F.; Qian, D.; Lin, J.; Hou, J.; Li, Y. High performance polymer solar cells with as-prepared zirconium acetylacetonate film as cathode buffer layer. *Sci. Rep.* **2014**, *4*, 4691.
39 Ju, H.; Zhu, Q. L.; Zuo, M.; Liang, S.; Du, M.; Zheng, Q.; Wu, Z. L. Toughening hydrogels by forming robust hydrazide-transition metal coordination complexes. *Chem. Eur. J.* **2023**, *29*, e202300969.
40 Chen, J.; Gao, Y.; Shi, L.; Yu, W.; Sun, Z.; Zhou, Y.; Liu, S.; Mao, H.; Zhang, D.; Lu, T.; Chen, Q.; Yu, D.; Ding, S. Phase-locked constructing dynamic supramolecular ionic conductive elastomers with superior toughness, autonomous self-healing and recyclability. *Nat. Commun.* **2022**, *13*, 4868.
41 Jiang, Y.; Zhan, D.; Zhang, M.; Zhu, Y.; Zhong, H.; Wu, Y.; Tan, Q.; Dong, X.; Zhang, D.; Hadjichristidis, N. Strong and ultra-tough ionic hydrogel based on hyperbranched macro-cross-linker: influence of topological structure on properties. *Angew. Chem. Int. Ed.* **2023**, *62*, e202310832.
42 Zhang, M.; Yang, Y.; Li, M.; Shang, Q.; Xie, R.; Yu, J.; Shen, K.; Zhang, Y.; Cheng, Y. Toughening double-network hydrogels by polyelectrolytes. *Adv. Mater.* **2023**, *35*, e2301551.
43 Hu, L.; Wang, Y.; Liu, Q.; Liu, M.; Yang, F.; Wang, C.; Pan, P.; Wang, L.; Chen, L.; Chen, J. Real-time monitoring flexible hydrogels based on dual physically cross-linked network for promoting wound healing. *Chinese Chem. Lett.* **2023**, *34*, 108262.
44 Fang, X.; Sun, J. One-step synthesis of healable weak-polyelectrolyte-based hydrogels with high mechanical strength, toughness, and excellent self-recovery. *ACS Macro Lett.* **2019**, *8*, 500–505.
45 Lin, P.; Ma, S.; Wang, X.; Zhou, F. Molecularly engineered dual-crosslinked hydrogel with ultrahigh mechanical strength, toughness, and good self-recovery. *Adv. Mater.* **2015**, *27*, 2054–2059.
46 Hu, X.; Vatankhah-Varnoosfaderani, M.; Zhou, J.; Li, Q.; Sheiko, S. S. Weak hydrogen bonding enables hard, strong, tough, and elastic hydrogels. *Adv. Mater.* **2015**, *27*, 6899–905.
47 Shen, J.; Dai, Y.; Xia, F.; Zhang, X. Role of divalent metal ions in the function and application of hydrogels. *Prog. Polym. Sci.* **2022**, *135*, 101622.
48 Wang, Y.; Xie, Y.; Xie, X.; Wu, D.; Wu, H.; Luo, X.; Wu, Q.; Zhao, L.; Wu, J. Compliant and robust tissue-like hydrogels via ferric ion-induced of hierarchical structure. *Adv. Funct. Mater.* **2023**, *33*, 2210224.
49 Lu, X.; Si, Y.; Zhang, S.; Yu, J.; Ding, B. *In situ* synthesis of mechanically robust, transparent nanofiber-reinforced hydrogels for highly sensitive multiple sensing. *Adv. Funct. Mater*. **2021,** *31*, 2103117.
50 Zheng, S.; Chen, X.; Shen, K.; Cheng, Y.; Ma, L.; Ming, X. Hydrogen bonds reinforced ionogels with high sensitivity and stable autonomous adhesion as versatile ionic skins. *ACS Appl. Mater. Interfaces* **2024**, *16*, 4035–4044.
51 Shen, K.; Liu, Z.; Xie, R.; Zhang, Y.; Yang, Y.; Zhao, X.; Zhang, Y.; Yang, A.; Cheng, Y. Nanocomposite conductive hydrogels with Robust elasticity and multifunctional responsiveness for flexible sensing and wound monitoring. *Mater. Horiz.* **2023**, *10*, 2096–2108.
52 Yuan, W.; Qu, X.; Lu, Y.; Zhao, W.; Ren, Y.; Wang, Q.; Wang, W.; Dong, X. MXene-composited highly stretchable, sensitive and durable hydrogel for flexible strain sensors. *Chinese Chem. Lett.* **2021**, *32*, 2021–2026.
53 Liu, Y.; Tian, G.; Du, Y.; Shi, P.; Li, N.; Li, Y.; Qin, Z.; Jiao, T.; He, X. Highly stretchable, low-hysteresis, and adhesive ta@mxene-composited organohydrogels for durable wearable sensors. *Adv. Funct. Mater.* **2024**, 2315813.
54 Wang, W.; Zhou, H.; Xu, Z.; Li, Z.; Zhang, L.; Wan, P. Flexible conformally bioadhesive mxene hydrogel electronics for machine learning-facilitated human-interactive sensing. *Adv. Mater.* **2024**, 2401035.